

| | |
|-----------------------------|--|
| Title | Silicon-based resonant-cavity-enhanced photodiode with a buried SiO ₂ reflector |
| Authors | Sinnis, Vasileios S.;Seto, M.;'t Hooft, G. W.;Watabe, Y.;Morrison, Alan P.;Hoekstra, W.;de Boer, W. B. |
| Publication date | 1999 |
| Original Citation | Sinnis, V. S., Seto, M., Hooft, G. W. t., Watabe, Y., Morrison, A. P., Hoekstra, W. and Boer, W. B. d. (1999) 'Silicon-based resonant-cavity-enhanced photodiode with a buried SiO ₂ reflector', Applied Physics Letters, 74(9), pp. 1203-1205. doi: 10.1063/1.123499 |
| Type of publication | Article (peer-reviewed) |
| Link to publisher's version | http://aip.scitation.org/doi/abs/10.1063/1.123499 - 10.1063/1.123499 |
| Rights | © 1999 American Institute of Physics.This article may be downloaded for personal use only. Any other use requires prior permission of the author and AIP Publishing. The following article appeared in Sinnis, V. S., Seto, M., Hooft, G. W. t., Watabe, Y., Morrison, A. P., Hoekstra, W. and Boer, W. B. d. (1999) 'Silicon-based resonant-cavity-enhanced photodiode with a buried SiO ₂ reflector', Applied Physics Letters, 74(9), pp. 1203-1205 and may be found at http://aip.scitation.org/doi/abs/10.1063/1.123499 |
| Download date | 2024-04-24 17:15:15 |
| Item downloaded from | https://hdl.handle.net/10468/4410 |

Silicon-based resonant-cavity-enhanced photodiode with a buried SiO₂ reflector

V. S. Sini¹, M. Seto² and G. W. 't Hooft³, Y. Watabe⁴, A. P. Morrison⁵, W. Hoekstra⁶ and W. B. de Boer⁷

Citation: *Appl. Phys. Lett.* **74**, 1203 (1999); doi: 10.1063/1.123499

View online: <http://dx.doi.org/10.1063/1.123499>

View Table of Contents: <http://aip.scitation.org/toc/apl/74/9>

Published by the [American Institute of Physics](#)



Silicon-based resonant-cavity-enhanced photodiode with a buried SiO₂ reflector

V. S. Sinnis^{a)}

National Microelectronics Research Centre, Lee Maltings Prospect Row, Cork, Ireland and Philips Research Laboratories, Prof. Holstlaan 4, 5656 AA Eindhoven, The Netherlands

M. Seto and G. W. 't Hooft

Philips Research Laboratories, Prof. Holstlaan 4, 5656 AA Eindhoven, The Netherlands

Y. Watabe

Philips Industrial Activities, Kempische steenweg 293, B-3500 Hasselt, Belgium

A. P. Morrison

National Microelectronics Research Centre, Lee Maltings Prospect Row, Cork, Ireland

W. Hoekstra and W. B. de Boer

Philips Research Laboratories, Prof. Holstlaan 4, 5656 AA Eindhoven, The Netherlands

(Received 30 September 1998; accepted for publication 23 December 1998)

We report on a silicon-based resonant cavity photodiode with a buried silicon dioxide layer as the bottom reflector. The buried oxide is created by using a separation by implantation of oxygen technique. The device shows large Fabry-Pérot oscillations. Resonant peaks and antiresonant troughs are observed as a function of the wavelength, with a peak responsivity of about 50 mA/W at 650 and 709 nm. The leakage current density is 85 pA/mm² at -5 V, and the average zero-bias capacitance is 12 pF/mm². We also demonstrate that the buried oxide prevents carriers generated deep within the substrate from reaching the top contacts, thus removing any slow carrier diffusion tail from the impulse response. © 1999 American Institute of Physics. [S0003-6951(99)02109-9]

Because of its indirect band gap, silicon has a very long absorption length, when compared to a direct band gap material such as GaAs. For example, at $\lambda = 700$ nm the silicon absorption constant is $\alpha = 3 \times 10^3 \text{ cm}^{-1}$, corresponding to an absorption length of $\alpha^{-1} = 3.3 \text{ } \mu\text{m}$.¹ As a consequence, typical silicon photodiodes require a large device thickness to achieve the requisite responsivity.² However, this can lead to a transit time limited bandwidth due to the long distance carriers have to travel. It has been shown that the tradeoff between bandwidth and responsivity can be circumvented by using a resonant cavity structure.³ The idea is to sandwich the absorption layer between two mirrors, so that light not absorbed in the first pass is reflected back into the active region. This effectively increases the absorption cavity thickness, while keeping the carrier transit distance the same. This approach has recently been used to demonstrate a silicon-based resonant cavity photodiode with a multilayer SiGe/Si Bragg mirror as the bottom reflector.^{4,5} However, the main problem with using a Si/SiGe Bragg mirror is the high leakage current caused by crystal defects arising from dislocations, due to the large lattice mismatch between the silicon and silicon-germanium layers.

Recently, there have been reports on a resonant cavity photodiode made on bond-and-etchback silicon-on-insulator (SOI) substrate,⁶ as well as SOI material made by the separation by implantation of oxygen (SIMOX) technique.⁷ Here, the silicon and buried SiO₂ interface is used as one of the mirrors. Using SOI material for a resonant cavity photodiode has a number of advantages compared to a multiple Si/SiGe Bragg mirror device. Because of the large index difference

between silicon ($n_{\text{Si}} = 3.8$ at 720 nm) and silicon dioxide ($n_{\text{SiO}_2} = 1.47$ at 720 nm), this single buried SiO₂ has a comparable reflectance to many Si/SiGe pairs. In general, a SOI wafer contains far fewer defects than that of a wafer with relaxed Si/SiGe layers. SOI wafers can also be subjected to high temperature treatment for dopant diffusions and anneals, as is used in conventional silicon processing technology. These high temperatures cannot be used with SiGe/Si mirrors due to interdiffusion of Ge in the Bragg stack. Carline *et al.*⁶ demonstrated a long-wavelength Si/SiGe quantum well infrared photodetector on a bond-and-etchback SOI substrate. In this letter, we report on a resonant-cavity lateral *p-i-n* photodiode made on SIMOX material, optimized for 722 nm wavelength. In addition to measuring the responsivity as a function of the wavelength, we also present results on the rise and fall times of the detector response, and show that the buried oxide layer has the advantage of removing slow carrier diffusion as well as being one of the resonant cavity mirrors.

Photodiodes were fabricated using commercially available SIMOX wafers⁸ (15 cm diameter (100) 15 $\Omega \text{ cm}$ *p* type) with an initial mean silicon surface thickness of 0.212 μm and a buried oxide thickness of 0.373 μm . This corresponds to a maximum internal reflectance of 54% at 722 nm. The quantum efficiency of a resonant cavity photodetector can be shown to be⁹

$$\eta = \left(\frac{1 + R_2 e^{-\alpha d}}{1 - 2\sqrt{R_1 R_2} e^{-\alpha d} \cos\left(\frac{4n\pi d}{\lambda} + \phi_1 + \phi_2\right) + R_1 R_2 e^{-2\alpha d}} \right) \times (1 - R_1)(1 - e^{-\alpha d}), \quad (1)$$

^{a)}Electronic mail: bsinnis@nmrc.ucc.ie

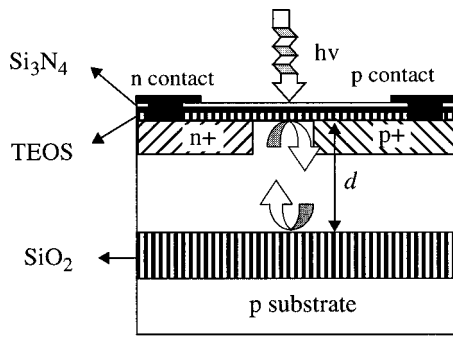


FIG. 1. Schematic cross sectional diagram of lateral *p-i-n* resonant cavity photodiode.

where η is the quantum efficiency, R_1 and R_2 are the top and bottom reflectances, α is the absorption coefficient, d is the cavity thickness, n is the index of refraction, λ is the wavelength of the incident light in vacuum, and ϕ_1 and ϕ_2 are phase shifts from reflections at the top and bottom mirrors. Knowing the bottom mirror reflectance, one can use this equation to calculate the optimal device cavity thickness for a desired wavelength.

Low temperature chemical vapor deposition (CVD) was used to grow 100 Ω cm *n*-type silicon on top of the SIMOX substrate to make a total thickness of $d = 0.96 \mu\text{m}$, where we calculated that this should provide resonant enhancement at 722 nm. Standard cleanroom photolithography techniques were used to define *n+* and *p+* regions, forming a lateral *p-i-n* diode. The top mirror is semitransparent and optimized to act as a semireflecting coating to allow as much light into the cavity as possible and still act as a mirror for the unabsorbed portion of light within the cavity. The top mirror reflectance gives the highest quantum efficiency when $R_1 = R_2 e^{-2\alpha d}$. With $R_2 = 54\%$ for the given buried oxide thickness and a cavity thickness of $0.96 \mu\text{m}$, the optimal value for R_1 is 38%, using $1/\alpha = 5.39 \mu\text{m}$ at 722 nm. In our structure, the top mirror consists of 82.65 nm tetraethylorthosilicate (TEOS) oxide and 70.65 nm silicon nitride, which we calculated to give an $R_1 = 40\%$. This resonant cavity photodetector can be tuned to the desired wavelength in order to maximize the responsivity by carefully adjusting the thickness of the layers. In our case, the design is such that the responsivity should be high at around 660 and 720 nm. A schematic cross section of the fabricated photodiode is shown in Fig. 1.

The responsivity of the photodiodes was measured as a function of the wavelength. A tungsten halogen lamp along with a grating monochromator was used in order to scan λ from 550 to 750 nm at 1 nm intervals. Fabry-Pérot oscillations are observed, as shown in Fig. 2 for two different devices as an indication of the resonant enhancement. The peak to trough difference is 290% and trough to trough $\Delta\lambda = 54$ nm about the peak at 709 nm. The responsivity at 709 nm is 49.1 mA/W, and is slightly higher at 658 nm with 51.6 mA/W. The peak at 658 nm is higher than at 709 nm due to a combination of resonant enhancement and higher absorption at shorter wavelengths. Using a transfer-matrix method to determine the reflectances at the various interfaces we calculate, without any fitting parameters and using only optical constants that can be found in the literature, a respon-

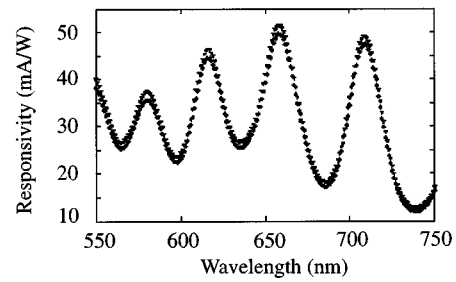


FIG. 2. Responsivity measurements of two different devices from the same wafer. Large Fabry-Pérot oscillations are evident, indicating resonant cavity enhancement.

sivity of 50 mA/W at 655 nm. This value matches well with what we measured.

Figure 3 shows a typical current-voltage (*I-V*) trace under forward and reverse bias. Good diode rectification characteristics are displayed with leakage current less than 1 nA in reverse, and rising 4 orders of magnitude at 0.5 V forward bias. In this case, the junction area is 0.7247 mm^2 . The average leakage current density was found to be 85 pA/mm² at -5 V. This is 2700 times less, at the same bias condition, than that for devices using a SiGe/Si Bragg mirror,⁵ due to the lower defect density. The zero bias capacitance per unit area was measured to be on the average of 12 pF/mm². This value is about four times less than the capacitance per area measured for vertical Si/SiGe Bragg mirror photodiodes, due to the lateral *p-i-n* structure.

High-speed temporal response measurements of the photodiodes were made. Figure 4 shows the response of the photodiode illuminated by a 17 ps long pulse from a dye laser tuned at 590 nm wavelength pumped by a mode-locked argon ion laser. The repetition rate was 8 MHz. The photodiode shows a rise time of 350 ps, full recovery fall time of 3.1 ns and a full width at half maximum equal to 660 ps. The photodiode was reverse biased at 27 V. A fast Fourier transform of this response into the frequency domain yields a $f_{3\text{ dB}}$ bandwidth of 427 MHz.

An important feature of this device is the buried oxide layer that limits the silicon active layer thickness and prevents carriers photogenerated in the substrate from reaching the electrodes. Only carriers photogenerated in the active SOI layer contribute to the photocurrent. Blocking carriers that are created deeper than the buried oxide from being collected could be of interest for applications where it is important to remove a slow diffusion tail from the photoreponse since carriers generated deep within the substrate require a long diffusion time to reach the electrodes. Figure 4 shows the response of a photodiode with a buried oxide in

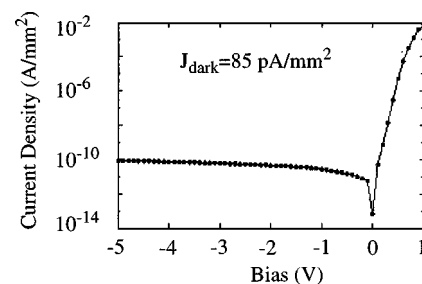


FIG. 3. *I-V* characteristic of a photodiode under forward and reverse bias.

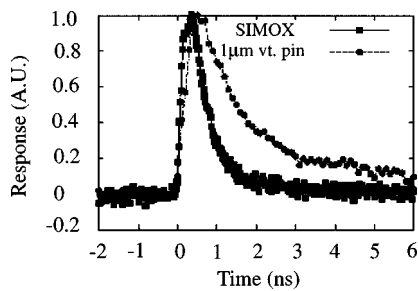


FIG. 4. Pulse response of SIMOX resonant cavity photodiode. For comparison, we also include the pulse response of a vertical p - i - n photodiode without the buried oxide. The vertical p - i - n photodiode has a much longer fall time due to a slow carrier diffusion tail due to photogeneration outside the depleted area.

comparison with a $1\text{ }\mu\text{m}$ active layer vertical photodiode without buried oxide. The SIMOX resonant cavity is clearly faster with a shorter fall time. At 590 nm wavelength, the silicon absorption length is greater than the cavity thickness, so that the oxide must be blocking slow carrier diffusion.

We did electric and potential field calculations using the commercial software package MEDICI¹⁰ in order to calculate the depletion region of the SIMOX diode structure. It was found that because the top n^+ and p^+ regions were separated by $20\text{ }\mu\text{m}$, the electric field at 27 V was not sufficiently high to induce electron and hole saturation velocities. In fact, most of the potential drop is across the n -type epitaxial material, and the buried oxide and lowly doped p -type substrate. These results show that faster photodiodes can be obtained by reducing the distance between the two highly doped regions. In future work, a redesign of the photomask should be done, for example, using interdigitated finger structures for the p^+ and n^+ areas, with spacing distance between the fingers comparable to or less than the thickness of the SOI layer.

In conclusion, a resonant cavity photodiode using a SIMOX wafer as base material has been demonstrated. Fabry-Pérot oscillation in the device responsivity were observed with a maximum responsivity of 50 mA/W at 658 nm and 49.1 mA/W at 709 nm . However, the maximum responsivity at the resonant wavelength for these devices is lower by a factor of 6 than that of the devices using SiGe/Si mirrors,⁵ since there is no contribution from SiGe layers and the substrate. The device cavity contains far fewer defects than devices using SiGe/Si mirrors so that it exhibits a much lower average leakage current density. There is a full width at half maximum response time of 660 ps . A fast Fourier transform of the impulse response yields $f_{3\text{ dB}} = 427\text{ MHz}$. Faster devices can be fabricated by reducing the lateral distance between the n^+ and p^+ regions.

The authors would like to thank H. G. R. Maas for his helpful advice.

- ¹P. J. Timans, in *Advances in Rapid Thermal and Integrated Processing*, edited by F. Roozeboom (Kluwer Academic, London, 1995).
- ²M. Seto, M. Mabeoone, S. de Jager, A. Vermeulen, W. de Boer, M. Theunissen, and H. Tuinhout, *Solid-State Electron.* **41**, 1083 (1997).
- ³A. Chin and T. Y. Chang, *J. Vac. Sci. Technol. B* **8**, 339 (1990).
- ⁴S. S. Murtaza, H. Nie, J. C. Campbell, J. C. Bean, and L. J. Peticolas, *IEEE Photonics Technol. Lett.* **8**, 927 (1996).
- ⁵M. Seto, W. B. de Boer, V. S. Sinnis, A. P. Morrison, W. Hoekstra, and S. de Jager, *Appl. Phys. Lett.* **72**, 1550 (1998).
- ⁶R. T. Carline, D. J. Robbins, M. B. Stanaway, and W. Y. Leong, *Appl. Phys. Lett.* **68**, 544 (1996).
- ⁷M. Seto, V. S. Sinnis, A. P. Morrison, W. Hoekstra, and W. B. de Boer, *28th ESSDERC* (Editions Frontieres, Paris, 1998), pp. 196–199.
- ⁸Ibis Technology Corporation, 32A Cherry Hill Drive, Danvers, MA 01923.
- ⁹M. S. Unlu and S. Strite, *J. Appl. Phys.* **78**, 607 (1995).
- ¹⁰MEDICI 2.2.1, Technology Modelling Associates, 595 N. Lawrence Expressway, Sunnyvale, CA 94086-3922.